Human hippocampal theta oscillations reflect sequential dependencies during spatial planning.

Raphael Kaplan[1,2], Adrià Tauste Campo[3-5], Daniel Bush[6,7], John King[6,8], Alessandro Principe[2], Raphael Koster[1,6], Miguel Ley-Nacher[3], Rodrigo Rocamora[3], & Karl J. Friston[1]

1-Wellcome Centre for Human Neuroimaging, UCL Institute of Neurology, University College London, 12 Queen Square, London, United Kingdom, WC1N 3BG.

2-Egil and Pauline Braathen and Fred Kavli Centre for Cortical Microcircuits, Kavli Institute for Systems Neuroscience, Norwegian University of Science and Technology, Olav Kyrres gate 9, Trondheim, Norway 7030

3-Center for Brain and Cognition, Department of Information and Communication Technologies, Universitat Pompeu Fabra, Edifici Merce Rodereda, C/ Ramón Trias Fargas, 25, Barcelona, Spain 08018.

4-Epilepsy Unit, Department of Neurology, Hospital del Mar Medical Research Institute (IMIM), Dr. Aiguader 88, Barcelona, Spain 08003.

5-Barcelonaβeta Brain Research Center, Pasqual Maragall Foundation, C/ Wellington 30, Barcelona, Spain 08005.

6-UCL Institute of Cognitive Neuroscience, University College London, 17 Queen Square, London, United Kingdom, WC1N 3AZ.

7- Institute of Neurology, University College London, London, United Kingdom, WC1N 3BG.

8- Clinical, Education and Health Psychology, University College London, 1-19 Torrington Place, London, United Kingdom, WC1E 7HB.

Corresponding Author: Raphael Kaplan; email: raphael.s.m.kaplan@ntnu.no, Egil and Pauline Braathen and Fred Kavli Centre for Cortical Microcircuits, Kavli Institute for

Systems Neuroscience, Norwegian University of Science and Technology Olav Kyrres gate 9, Trondheim, Norway 7030

Manuscript information: This manuscript contain 28 pages (Abstract: 172 words, Introduction: 602 words, Discussion: 1413 words), 5 Figures, and 1 Table.

Conflict of interest: The authors declare no competing financial interests.

Acknowledgements: The research was supported by a Sir Henry Wellcome Postdoctoral Fellowship to RKa (Ref: 101261/Z/13/Z) and a Wellcome Principal Research Fellowship to KJF (Ref: 088130/Z/09/Z). We thank Carmen Pérez Enríquez for helpful discussion and the staff at Hospital del Mar for help with patients. We would also like to thank David Bradbury and Letty Manyande for assistance with MEG experimental setup. We also thank the Wellcome Centre for Human Neuroimaging for providing facilities.

Abstract

Movement-related theta oscillations in rodent hippocampus coordinate ‘forward sweeps’ of location-specific neural activity that could be used to evaluate spatial trajectories online. This raises the possibility that increases in human hippocampal theta power accompany the evaluation of upcoming spatial choices. To test this hypothesis, we measured hippocampal oscillations during a spatial planning task that closely resembles a perceptual decision-making paradigm. In this task, female and male participants searched visually for the shortest path between a start and goal location in novel mazes that contained multiple choice points, and were subsequently asked to make a spatial decision at one of those choice points. During the search/planning period, we observed ~3-6 Hz hippocampal theta power increases that were negatively correlated with subsequent decision speed, where decision speed correlated with choice accuracy. Notably, hippocampal theta power increases were preferentially induced by planning in mazes containing a sequence of choices that were initially straightforward and subsequently ambiguous. These results implicate the hippocampal theta rhythm in the searches of deep decision trees, with a particular ‘bottleneck’ form.

Significance Statement

Low frequency (~<10 Hz) hippocampal theta oscillations are putatively linked with learning and decision-making in rodents, but how hippocampal theta relates to specific decision processes is unclear. Here, we tested human volunteers on a spatial planning paradigm that discloses the role of the hippocampal theta rhythm when planning sequential choices in novel environments. Recording from the human hippocampus, we find that increased hippocampal theta power correlates with planning quicker and more accurate spatial decisions. Furthermore, hippocampal theta power increased during planning in mazes with choice sequences that were initially straightforward and subsequently ambiguous. These results implicate the human hippocampal theta rhythm in the evaluation of demanding upcoming spatial choices.

Introduction

Human hippocampal theta oscillations have been linked to memory performance (Cornwell et al., 2008; Guderian et al., 2009; Poch et al., 2011; Kaplan et al., 2012; Lega et al., 2012; Olsen et al., 2013; Staudigl & Hanslmayr, 2013; Watrous et al., 2013; Backus et al., 2016; Heusser et al., 2016) and confidence in decisions (Guitart-Masip et al., 2013; Oehrn et al., 2015; Khemka et al., 2017). Although memory performance and decision confidence are important when making effective memory-guided decisions, it remains unclear whether changes in hippocampal theta power are associated with specific aspects of decision-making. Notably, rodent type I movement-related hippocampal theta oscillations (Vanderwolf, 1969) are linked to sweeps of place cell activity produced by hippocampal theta phase precession (O'Keefe & Recce, 1993). It has been hypothesized that phase precession could therefore serve as a mechanism to plan trajectories online (Johnson & Redish, 2007; Buzsáki & Moser, 2013; Wikenheiser & Redish, 2015; Watrous et al., 2018). This raises the possibility that similar increases in human hippocampal theta power are induced by the planning of forward trajectories.

To investigate the role of the hippocampal theta rhythm in online spatial planning (i.e., the search of deep decision trees), we created a spatial task that required little to no learning, in which participants could draw upon their experience in the physical world (Kaplan et al., 2017a). We tested human participants on this task, while recording from the hippocampus either invasively, using intracranial electroencephalography (iEEG); or non-invasively, using whole-head magnetoencephalography (MEG). In both cases, participants were instructed to search for the shortest path between a start and goal in novel mazes that afforded multiple paths. Participants were then asked which direction they would take from one of two choice points along the shortest path (Fig. 1).

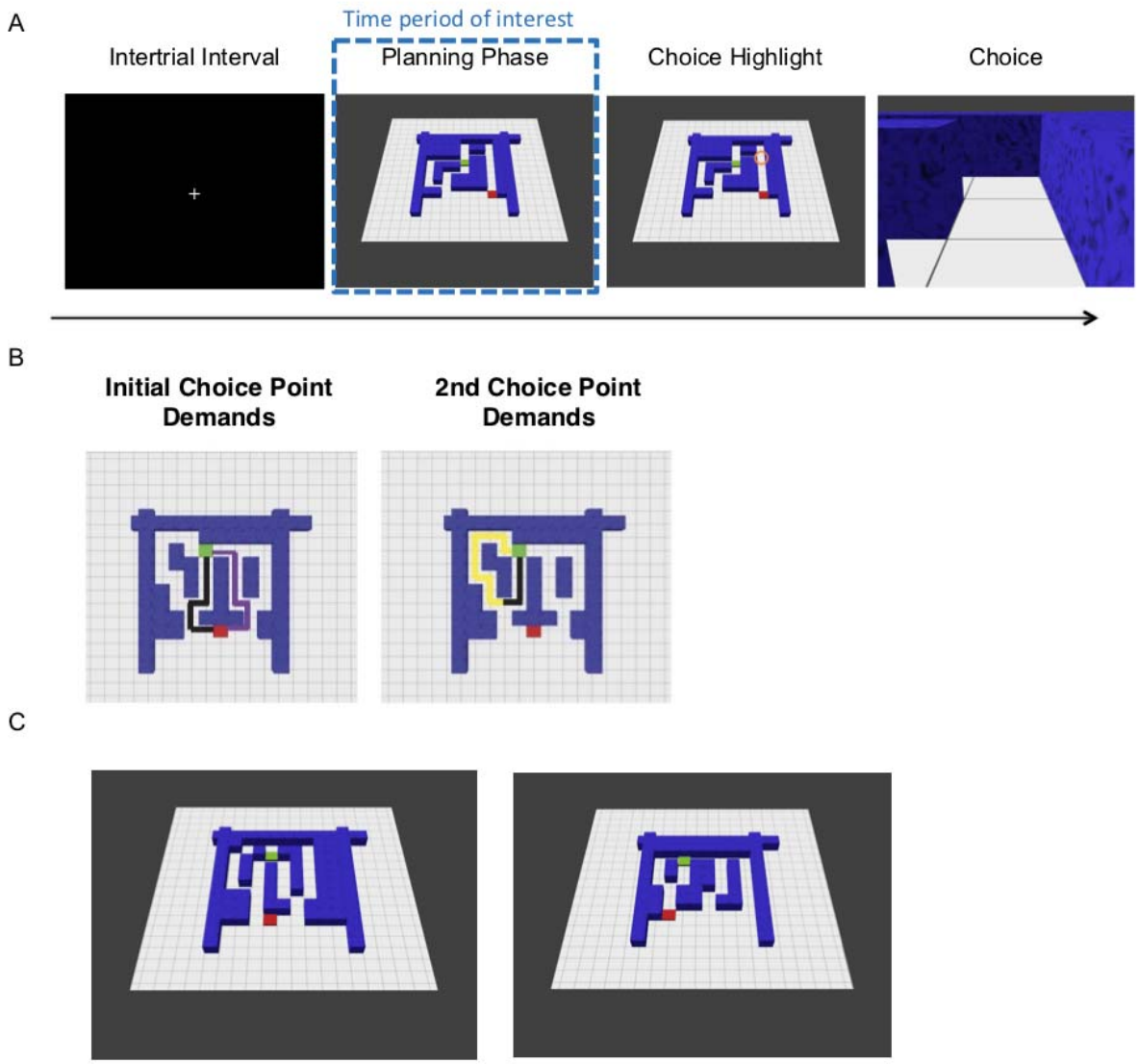

Fig 1. Task. A. Each trial (i.e., visually presented maze) began with an inter-trial interval (ITI) of 1.5s. Next, during a 3.25s planning phase, participants had to infer the shortest path from a start point (red square) to a goal location (green square) and remember the chosen direction for each choice point along the shortest path. A choice point was subsequently highlighted (choice highlight) for 250ms. This was either the first (i.e. initial) or second (i.e. subsequent) choice point along the shortest path. Participants were then asked which direction (e.g., left or forward) they would take at that choice point – during a choice period that was cued by a first-person viewpoint of the highlighted location. Participants had a maximum of 1.5 s (MEG) or 2 s (iEEG) to make their choice using a button box. B. Overhead view (not shown during the experiment) of two example mazes, indicating which path lengths contribute to each condition. C. Left: Example trial with a small path length difference (demanding) at the red square/initial choice point and large (less demanding) path length difference at the second choice point. Right: Example trial with a large (less demanding) path length difference at the red square/initial choice point and small (demanding) path length difference at the second choice point.

Crucially, the mazes were designed to induce forward planning in terms of a deep, two-level tree search, where participants needed to maintain the decisions they made at each choice point. At both choice points, there was a small, medium, or large path length difference – creating a total of (3x3) nine conditions allowing us to test the effect of choice point depth (i.e., initial or second) on planning demands (small, medium or large). We associate a smaller path difference with greater ambiguity and processing demands. Importantly, participants were only prompted to make one choice after seeing the full maze; however, until the choice point was highlighted, they did not know which decision (i.e. either the initial or second/subsequent choice point along the correct path) would be probed (Fig. 1). After planning their route, participants were asked to choose—at a specified choice point—the direction of the shortest path to the goal location (Fig. 1). This provided a measure (reaction time, RT) with which to quantify their (subjective) uncertainty to complement the (objective) difference in path lengths. This design allowed us to ask whether hippocampal theta power is selectively related to demands at specific choice points and how the theta rhythm relates to successful sequential spatial planning.

In brief, we observed a task-related increase in 3-6 Hz hippocampal theta power during the planning phase in our iEEG recordings, which was used as a frequency window of interest to analyze our MEG data. We found that hippocampal theta power increases during this period correlated with shorter reaction times in both iEEG and MEG datasets, where decision speed also correlated with choice accuracy. Focusing on the MEG dataset – to definitively link hippocampal theta power changes to planning – we found that hippocampal theta power increases were preferentially induced during the planning of routes through mazes that contained straightforward initial choices and demanding subsequent choices.

Materials and Methods

Participants

MEG

Twenty-four participants (14 female: mean age 23.5 yrs; SD of 3.49 years) gave written consent and were compensated for performing the experimental task, as approved by the local research ethics committee at University College London in accordance with Declaration of Helsinki protocols. All participants had normal or corrected-to-normal vision and reported to be in good health with no prior history of neurological disease. Due to technical difficulties, two participants were removed from our sample, leaving twenty-two participants in the behavioral and MEG analyses presented here.

iEEG

Pre-surgical EEG recordings from 2 patients with pharmacoresistant focal-onset seizures and hippocampal depth electrodes gave written consent, as approved by the local ethics committee at Hospital del Mar and in accordance with Declaration of Helsinki protocols. One patient was removed from analyses, because of visual difficulties due to an inferior occipital lesion, leaving one patient with normal vision presented in the current analysis. A summary of the patient's characteristics is given in Table 1.

Age/ Sex	Handedness	Seizure Onset/Freq	Education	Epileptic Focus	Drugs & Dosage	First-language
23M	R (but used L due to IV)	16 yo (1 seizure per week and now seizure free)	Secondary	R Temporobasal (temporal pole)	Eslicarbazepinole 1000 mg/per day; leviteracetam 1500/2x day; Perampanel 8 mg/per day	Spanish

Table 1. Patient information

Patients were stereotactically implanted with depth electrodes for invasive presurgical diagnosis using a stereotactic ROSA robotic device (Medtech, France). All diagnostic and surgical procedures were approved by the clinical ethics committee of Hospital del Mar in accordance with the principles expressed by the Declaration of Helsinki. Electrode locations were determined solely by clinical criteria, ascertained by visual inspection of post-implantation MRI scans using Slicer 4 (Fedorov et al., 2012; www.slicer.org) and verified by an fMRI expert (R.Ka.). Patients were seizure free for at least 24 h before participation and

underwent an extensive neuropsychological evaluation to check for any cognitive impairments.

Experimental Design

Stimuli were presented via a digital LCD projector on a screen (height, 32 cm; width, 42 cm; distance from participant, ~70 cm) inside a magnetically shielded room using the Cogent (http://www.vislab.ucl.ac.uk/cogent.php) toolbox running in MATLAB (Mathworks, Natick, MA, USA). Over the course of 220 trials, participants viewed 220 different mazes from a slightly tilted (overhead) viewpoint and later chose from first-person viewpoints within mazes generated using Blender (http://www. blender.org). All mazes had a starting location (a red square) towards the bottom of the maze and a goal location (a green square) further into the maze (Kaplan et al., 2017a). Mazes differed by hierarchical depth (number of paths to a goal location): there were 110 mazes with four possible routes (sequential/deep mazes) and a further 110 non-sequential control mazes with two possible routes (shallow mazes) that were not included in the analyses presented in this study.

In the scanner, participants were first presented with pictures of novel mazes (Fig. 1) of varying difficulty (from an overhead viewpoint) and then asked to determine the shortest path from a starting location (a red square) at the bottom of the screen to the goal location (a green square). The overhead view appeared on the screen for 3.25 s, after which a location (choice point) along the path was highlighted briefly for 250 ms with an orange circle. The choice point location could either be the starting location or a second (subsequent) choice point. Crucially, participants would only have to make a decision about one choice point for each trial.

At either choice point, it was necessary to choose between two possible directions, which could be left, forward, or right, with an additional option to select equal, if both routes were the same distance. No second choice points with two incorrect choices were ever highlighted, only a second choice point along the optimal path after the starting location could be highlighted (Kaplan et al., 2017a). After the choice point was highlighted, a “zoomed in” viewpoint of this location (always one square back and facing the same direction as the

overhead viewpoint) was presented. Depending on the possible direction at the location, participants had less than 1,500 ms (2,000 ms for the iEEG patient) to decide whether to go left, forward, right, or occasionally either direction. If no button press was made within the allotted duration, the trial counted as an incorrect trial and the experiment moved on to the 1500-ms inter-trial interval (ITI) phase. Participants never received any feedback or reward for making the correct choice. As soon as participants chose a direction, the ITI phase of a trial began. Participants repeated this trial sequence 110 times per session, for a total of two sessions. Sessions lasted approximately 10–15 min. Session order was counterbalanced between participants.

All participants completed a brief practice session consisting of 40 mazes/trials before the experiment (on a laptop outside of the scanner). Deep/sequential mazes contained two branch/choice points between routes further in the maze, and the path length to reach the two choice points further in the maze was always equal. Mazes had square tiled floors and were 8 x 8, 9 x 9, or 10 x 10 squares in total area. In sequential/deep mazes, we used a 3x3 factorial design. Path length differences were split between 2 (small difference), 4 (medium difference), or 6 (large difference) squares (for an example, see square tiles in the mazes presented in Fig 1) for the two paths at the starting location and a path length difference of 2, 4, or 6 squares at the optimal choice point in the maze. There was one catch trial for deep/sequential and shallow/control mazes in each session, each containing all equal path lengths (path length differences of 0). In sum, sequential maze trials could be 2, 2; 2, 4; 2, 6; 4, 2; 4, 4; 4, 6; 6, 2; 6, 4; 6, 6; (e.g. 4, 2 would have a medium path length difference of 4 at the starting location, whereas the second choice point would have a small path length difference of 2). Half of the trials in the experiment were control/shallow mazes, which only contained one choice point at the red starting square. Data from these trials were not presented in the analyses presented in this study. For these mazes, path length differences were split between 2, 4, and 6, with one catch trial per session having equal path lengths.

iEEG recordings and artifact detection

All recordings were performed using a standard clinical EEG system (XLTEK, subsidiary of Natus Medical, Pleasanton, CA) with a 500 Hz sampling rate. A unilateral implantation was performed accordingly, using 15 intracerebral electrodes (Dixi Médical, Besançon, France; diameter: 0.8 mm; 5 to 15 contacts, 2 mm long, 1.5 mm apart) that were stereotactically inserted using robotic guidance (ROSA, Medtech Surgical, New York, NY).

Intracranial EEG signals were processed in the referential recording configuration (i.e., each signal was referred to a common reference; Tauste Campo et al., 2018). All recordings were subjected to a zero phase, 400th order finite impulse response (FIR) band-pass filter to focus on our frequency range of interest (0.5-48 Hz) and remove the effect of alternating current (Bush et al., 2017). Audio triggers produced by the stimulus presentation laptop were recorded on the monitoring system, allowing the EEG to be aligned with task information sampled at 25 Hz.

Analysis of EEG recordings focused on the 3.25 s planning periods with an additional 1.5 s baseline prior to trial onset (ITI period). All trials that included interictal spikes (IIS) or other artifacts, either within the period of interest or during the padding windows, were excluded from all analyses presented here. A 500 ms padding window was used at either end of planning period time series to minimize edge effects in subsequent analyses.

iEEG Time-Frequency Analysis

Estimates of dynamic oscillatory power during periods of interest were obtained by convolving the EEG signal with a seven-cycle Morlet wavelet and squaring the absolute value of the convolved signal. The wavelet transform was preferred to the Fourier transform as it does not assume stationarity in EEG recordings. To generate power spectra, the mean of dynamic oscillatory power estimates was taken over the time window of interest across the deepest contact in each hippocampal electrode. To perform baseline correction on time–frequency data for display purposes, power values were averaged across ITI periods for each frequency band, and those average values were subtracted from the power values at each time point in the planning period (Bush et al., 2017). To examine changes in oscillatory power within specific frequency bands and assess correlations among oscillatory power in each trial

with RT, dynamic estimates of oscillatory power were calculated over the time and frequency windows of interest. Power values were then averaged across hippocampal contacts to provide a single value at each time and frequency point for the patient.

MEG recording and preprocessing

Data were recorded continuously from 274 axial gradiometers using a CTF Omega whole-head system at a sampling rate of 600 Hz in third-order gradient configuration. Participants were also fitted with four electroculogram (EOG) electrodes to measure vertical and horizontal eye movements. MEG data analysis made use of custom made Matlab scripts, SPM8 &12 (Wellcome Centre for Human Neuroimaging, London), and Fieldtrip (Litvak et al., 2011; Oostenveld et al., 2011). For preprocessing, MEG data was epoched into 2s baseline periods prior to the planning phase for each of the nine sequential planning conditions of interest and the three non-sequential planning control conditions. Trials were visually inspected, with any trial featuring head movement or muscular artefacts being removed.

MEG Source Reconstruction

The linearly constrained minimum variance (LCMV) scalar beamformer spatial filter algorithm was used to generate source activity maps in a 10-mm grid (Barnes et al., 2003). Coregistration to MNI coordinates was based on nasion, left and right preauricular fiducial points. The forward model was derived from a single-shell model (Nolte, 2003) fit to the inner skull surface of the inverse normalized SPM template. The beamformer source reconstruction algorithm consists of two stages: first, based on the data covariance and lead field structure, weights are calculated which linearly map sensor data to each source location; and second, a summary statistic based on the mean oscillatory power between experimental conditions is calculated for each voxel.

Due to the proximity of frontal and anterior medial temporal lobe regions to the eyes, we wished to control for any possible influence of EOG muscular artefacts during the planning phase on estimates of oscillatory power. We therefore computed the variance of two

simultaneously recorded EOG signals across each planning phase and removed any covariance between these EOG variance values and oscillatory power measurements across voxels by linear regression (Kaplan et al., 2014, 2017c). This left 'residual' oscillatory power measurements for all trials whose variance could not be accounted for by changes in the EOG signal between trials, and these residual values were used as summary images for subsequent analyses. RT was included as an additional nuisance regressor for the theta power source analysis investigating the effect of path length differences at different choice points. Including RT as a nuisance regressor specifically for this analysis helped determine whether there were any residual hippocampal theta power effects related to choice point demands during the planning phase.

Statistical Analyses

There were two main periods of interest, the 1.5s ITI and 3.25s planning phase. For each of the 9 sequential planning regressors of interest (i.e., maze with a small, medium, or large path length at the second and first choice points), there were parametric regressors based on RT and accuracy (whether the choice was correctly answered; 1=incorrect choice; 2=correct choice). Inferences about these effects were based upon t- and F-tests using the standard summary statistic approach for second level random effects analysis.

A peak voxel significance threshold of $p<0.05$ FWE corrected for multiple comparisons was used for MEG source analyses. All images are displayed at the $p<0.001$ uncorrected threshold for illustrative purposes. Additionally, only clusters containing a significant peak voxel are displayed.

Post hoc statistical analyses were conducted using 10-mm radius spheres around the respective peak voxel specified in the GLM analysis. This allowed us to compare the effects of different regressors of interest (e.g., to determine whether a second choice point demand effect was present in a region defined by an orthogonal main effect of RT). This ensured we did not make any biased inferences in our post hoc analyses.

Results

Behavioral Performance

Participants in the MEG study made correct choices on 87.9 ± 6.13% of trials (mean ± SD; iEEG: 95.5%), with an average reaction time (RT) of 469 ± 99ms (iEEG: 423 ± 123ms). RTs were highly correlated with accuracy across MEG participants ($t(21)=-5.72$; $p<0.001$). In other words, participants responded faster when they made accurate choices. Moreover, this correlation showed that RT directly related to accurate performance on the spatial planning task. A similar correlation was not calculated for the iEEG patient due to the small number of incorrect trials.

We then asked whether accuracy and RT were specifically influenced by path length differences and choice point depth. This analysis allowed us to separate the effect of first/initial versus second/subsequent choice point demands on planning accuracy and RT. Using a repeated measures ANOVA (path length difference by choice point depth), we tested for an effect of path length difference on accuracy and RTs in MEG participants. We observed a significant interaction between initial (i.e. first) and second (i.e. subsequent) choice points and path length differences on both accuracy ($F(4,18)=11.0$; $p<0.001$) and RTs ($F(4,18)=4.75$; $p=0.009$). We found that accuracy was significantly related to path length differences at the first choice point ($F(2,20)=7.75$; $p=0.003$; Fig. 2A), where larger path length differences yielded better performance. However, no such relationship was observed with RTs ($F(2,20)=9.46$; $p=0.087$; Fig. 2B). Notably, we observed a significant effect of path length differences at the second choice point for both accuracy ($F(2,20)=15.0$; $p=0.001$; Fig. 2A) and RTs ($F(2,20)=14.0$; $p<0.001$; Fig. 2B). In contrast with behavioral responses at the initial choice point, second/subsequent choice point effects were more consistent: accuracy increased with greater path length differences, along with concomitant decreases in RT (see Figure 2). Noticeably, paired t-tests revealed that medium path length differences were significantly less demanding (i.e. higher accuracy and faster RT) when they were at the initial, as opposed to the second choice point (Accuracy: $t(21)=3.62$; $p=.002$; RT: $t(21)=-4.17$; $p<.001$; Fig. 2).

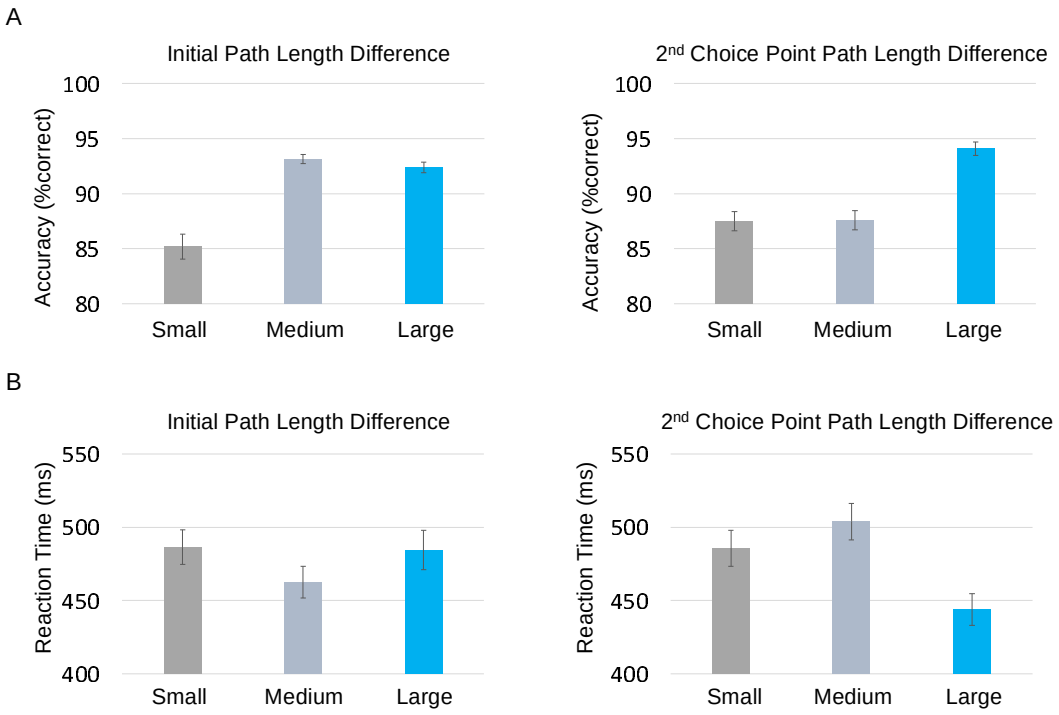

Figure 2: Behavior A. Accuracy. Left: Significant effect (p=0.003) of choice accuracy by first choice point path length differences, collapsed across second choice point path length differences (small, medium, and large). Right: Significant effect (p=0.001) of choice accuracy by second choice point path length differences, collapsed across initial path length differences (small, medium, and large). B. Reaction times. Left: Reaction time by initial choice point path length differences, collapsed across second choice point path length differences (small, medium, and large). Right: Significant effect (p<0.001) of reaction times by second choice point path length differences, collapsed across initial path length differences (small, medium, and large). All error bars show ± SEM.

Hippocampal depth recordings

Next, we examined changes in low frequency oscillatory power during the 3.25s planning period using iEEG recordings from depth electrodes located in the hippocampus of a single high performing pre-surgical epilepsy patient (Fig. 3A). Interestingly, a hippocampal theta rhythm was readily visible in the raw iEEG traces during this planning phase (Fig. 3B). In addition, the ensuing power spectrum (averaged across all trials) exhibited a prominent peak around ~4.5 Hz (Fig. 3C). Hence, we subsequently defined a theta frequency band of interest for our MEG analyses as a 3Hz frequency band centered on this peak (i.e. 3-6Hz).

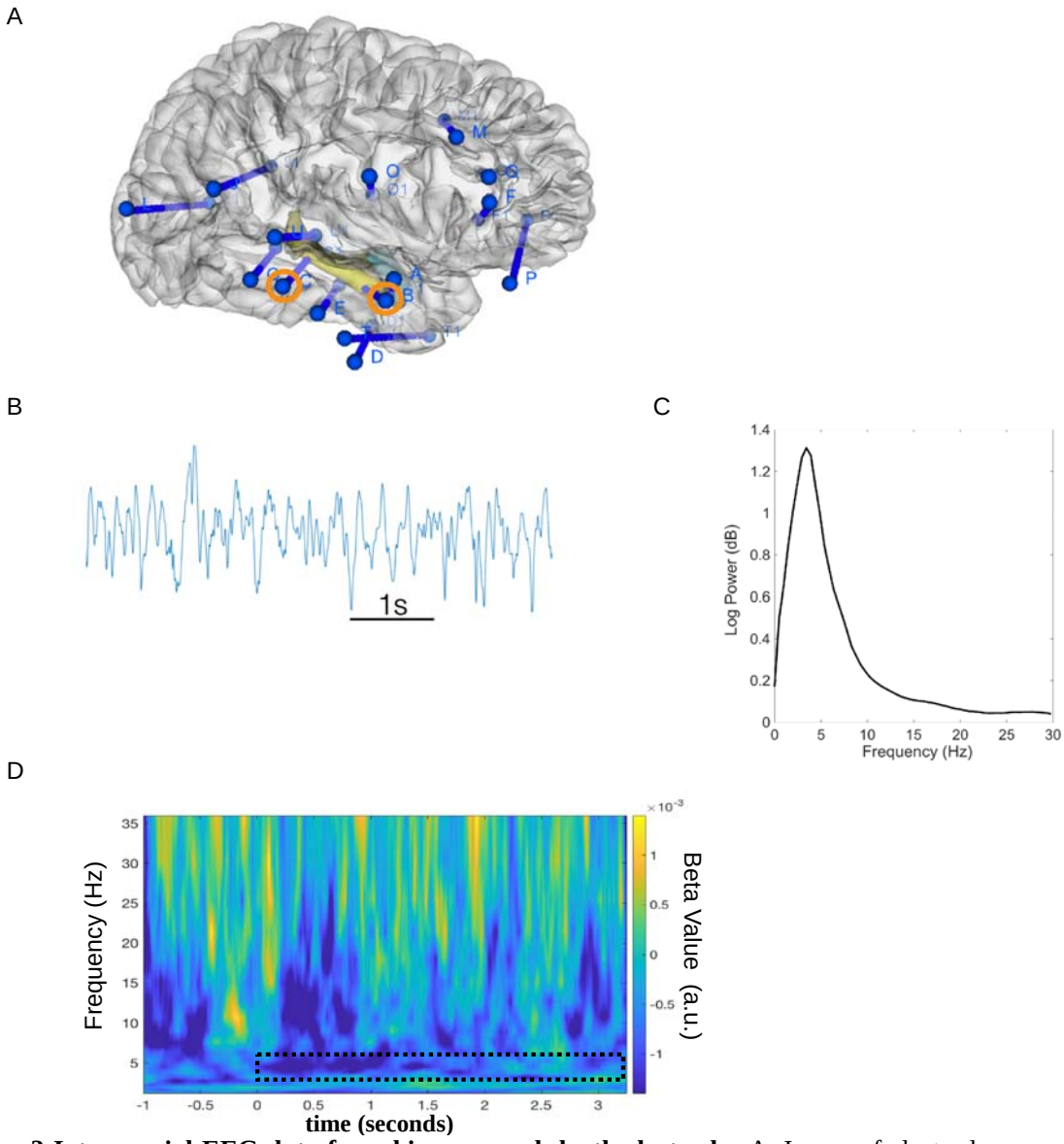

Fig. 3 Intracranial EEG data from hippocampal depth electrodes A. Image of electrode locations in the patient overlaid on 3D brain template. Right hippocampal depth electrodes with contacts used in the present analyses are highlighted in orange. B. Sample raw trace showing prominent ongoing theta band oscillations during the spatial planning task. C. Power spectrum centered on 3-6 Hz averaged across hippocampal contacts and trials. D. Time-frequency plot showing a negative correlation over trials between subsequent reaction time (RT) and 3-6 Hz theta power during planning phase (highlighted with dotted black box) averaged across hippocampal contacts.

Next, we asked whether hippocampal theta power during the planning phase correlated with the patient's subsequent performance on each trial. Interestingly, we observed a negative correlation between ~3-6 Hz hippocampal theta power and subsequent RT; i.e. increased hippocampal theta power during planning periods that preceded faster decisions (Fig. 3D).

Mean 3-6Hz theta power during the 3.25s planning phase correlated with trial by trial RTs ($r=-0.194; p=.043$), although this result should be interpreted with caution; given the relatively small number of measurements. On a related note, given the patient's relative lack of incorrect trials (5/110), we were unable to ask whether theta power increases correlated with accuracy. Overall, we observed hippocampal oscillations during the planning period that were most prominent between 3-6 Hz and exhibited power increases in the same frequency band that correlated with faster subsequent RT. Consequently, our iEEG findings allowed us to identify key data features for our MEG analyses. First, we focused on replicating the 3-6 Hz hippocampal theta RT effect in a larger sample. We then determined whether specific planning demands, in the form of particular path length differences at initial and second/subsequent choice points, contributed to this effect.

MEG Analyses

Using MEG source reconstruction, we asked whether changes in theta power were induced by spatial planning in a larger sample. We first examined the relationship between 3-6Hz theta power and RTs across the whole brain. Consistent with our finding of a correlation between hippocampal theta power during the planning phase and subsequent RTs in a single intracranial data set, we found a significant negative correlation between 3-6Hz power and RTs in a left hippocampal cluster (x:-20, y:-26, z:-16, $t(21)=-7.90$; family-wise error (FWE) corrected peak-voxel $p<0.001$; Fig. 4), but nowhere else in the brain. We then checked to see if this effect was also evident at the scalp level. We observed a similar effect at the scalp level, where frontal and left temporal sensors exhibited a negative correlation between 3-6 Hz theta power and RT (Fig. 4). We did not observe a significant positive correlation between 3-6 Hz planning period theta power and subsequent RTs elsewhere in the brain.

We then determined whether the RT effect was associated with a general increase in hippocampal theta power during spatial planning. Using a 10mm sphere around the left hippocampal peak, we observed a significant increase in hippocampal theta power in this region during the planning phase versus the ITI period ($t(21)=3.60; p=.002$; Fig. 4C).

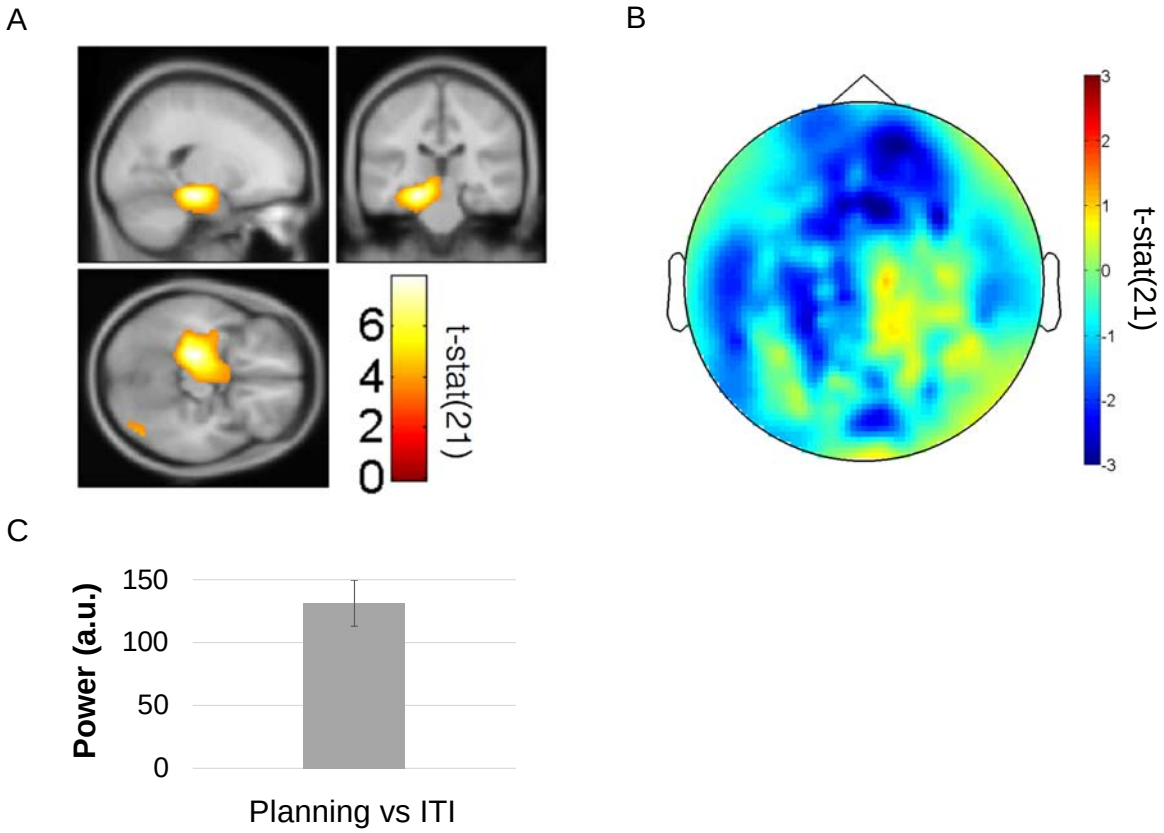

Fig. 4 Reaction time correlation with MEG theta power.
A. Linearly Constrained Minimum Variance (LCMV) beamformer source reconstruction images showing significant 3-6 Hz left hippocampal theta power source negative correlation with RT (x:-20, y:-26, z:-16, Z-score: 5.32; FWE peak-voxel $p<0.001$) in 22 healthy participants. Images displayed at the threshold of $p<0.001$ uncorrected. B. Negative 3-6 Hz theta power correlation with RT shown at the scalp level for 22 healthy participants. C. Data from a 10 mm sphere around left hippocampal peak voxel from RT contrast showing increased theta power during planning phase versus the ITI period. All error bars show ± SEM.

Isolating hippocampal theta power changes, we tested for the effects of processing demands (path length differences) at initial and second/subsequent choice points (e.g., quicker RT for mazes with less demanding initial choice points). For this analysis, we removed any covariance in theta power associated with RT over trials, which allowed us to determine whether there was a distinct hippocampal theta power effect induced by mazes affording less demanding path length differences, or a pruning of the search space to focus on specific demands at initial or second choice points. Using a repeated measures ANOVA (path length difference by choice point depth), we tested whether the left hippocampal region (exhibiting a theta power correlation with RT) also showed an effect of path length differences at initial

versus second choice points. In the left hippocampal theta power peak, we observed a significant interaction between path length difference and choice point depth (F(4,18)=5.88; p=0.003; Fig. 5A). Specifically, there were significant left hippocampal theta power effects related to both initial (F(2,20)=4.4;p=.026; Fig. 5) and second choice point differences in path length (F(2,20)=6.59;p=.006; Fig. 5). Paired t-tests revealed that hippocampal theta power was significantly higher (t(21)=3.83; p<.001) for medium path length differences at the second versus initial choice point, while large path length differences exhibited the opposite effect (t(21)=-6.09; p<.001; Fig. 5B-C). In other words, hippocampal theta power increases were generally related to planning in mazes with straightforward initial and demanding subsequent choices. One notable exception to this was higher hippocampal theta power for mazes with large path length differences at both choice points (i.e. very straightforward mazes).

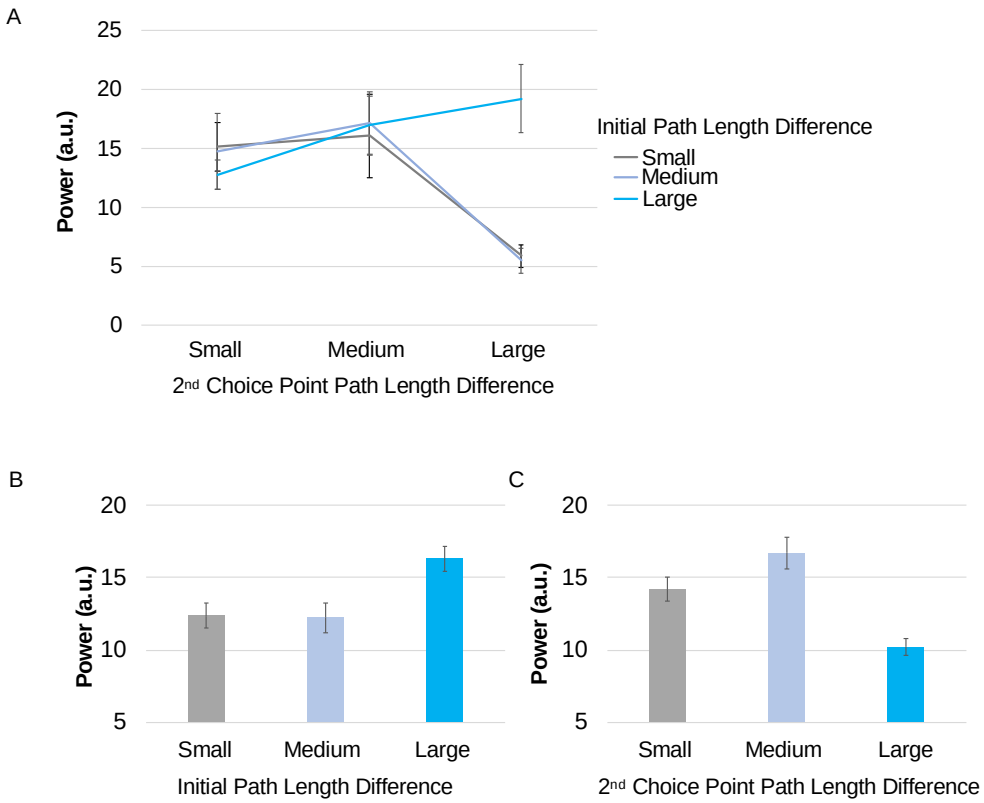

Fig. 5 Hippocampal theta power relates to specific choice point demands.
A. Significant interaction (p=.003) between initial and second/subsequent choice point path length differences for 10 mm sphere around hippocampal theta power peak voxel (that correlated with RT). B. Significant change in left hippocampal theta power by initial path length differences (p=.026) collapsed across second choice point path length (small, medium,

and large). C. Significant change in left hippocampal theta power related to second choice point path length differences (p=.006) collapsed across initial path length (small, medium, and large).

When testing for theta power effects related to path length differences and choice point depth across the whole brain, we did not observe any other significant effect of path length difference by choice point depth. Finally, we did not observe any correlation between theta power and trial-by-trial choice accuracy anywhere in the brain, although this is likely due to a relatively small number of errors.

Discussion

Using iEEG and MEG recordings during a spatial planning paradigm (Fig. 1), we examined how the human hippocampal theta rhythm relates to planning sequential decisions in novel environments. We first used hippocampal iEEG recordings to constrain our MEG analyses and observed ongoing 3-6 Hz hippocampal theta oscillations during spatial planning (Fig. 3). Linking hippocampal theta to participants' performance, hippocampal theta power during the planning phase correlated with faster subsequent spatial decisions in iEEG and MEG participants (Fig. 4). Furthermore, decision speed correlated with choice accuracy. Linking the human hippocampal theta rhythm to processing demands, we found that hippocampal theta power increased during planning in mazes with straightforward initial and demanding subsequent choices (Fig. 5). Here, we relate our findings to the extant hippocampal decision-making literature and speculate on potential computational roles associated with the hippocampal theta rhythm.

Our observation of increased hippocampal theta power during spatial decision-making adds to an emerging literature investigating the role of the hippocampal theta rhythm during decision-making in rodents (Johnson & Redish, 2007; Schmidt et al., 2013; Belchior et al., 2014; Wikenheiser & Redish, 2015; Pezzulo et al., 2017) and humans (Guitart-Masip et al., 2013; Oehrn et al., 2015). Yet, the specific role of the hippocampal theta rhythm in planning has remained unclear; despite recent evidence relating the rodent (Miller et al., 2017) and human hippocampus (Kaplan et al., 2017a) to planning. Further support for a

hippocampal role in planning comes from evidence that hippocampal neurons code the distance to goal locations (Ekstrom et al., 2003; Villette et al., 2015; Sarel et al., 2017; Watrous et al., 2018). Furthermore, Wikenheiser and Redish (2015) found that firing of place cell sequences coupled to the hippocampal theta rhythm extended further on journeys to distal goal locations. Paralleling these findings, we find hippocampal theta power was selectively related to evaluating straightforward initial choices and demanding subsequent choices. Taken together, these data implicate the hippocampal theta rhythm in goal-directed sequential planning.

Differing from previous MEG/iEEG hippocampal theta studies that observe power increases related generally to enhanced task performance (Lega et al., 2012; Olsen et al., 2013; Backus et al., 2016; Heusser et al., 2016), we find hippocampal theta power effects associated with both choice accuracy and spatial planning in mazes that involve easier initial and demanding subsequent choices. Given the known relationship between the hippocampal theta rhythm and spatial trajectories, these findings may relate to sequential spatial decision-making that focuses on an upcoming bottleneck along the optimal route – signifying a 'location' update within a sequence of choices. Supporting this explanation, models of the hippocampal formation have portended a role for the theta rhythm in encoding and parcellating the ordinal structure of the world in both spatial and abstract domains (Friston & Buzsaki, 2016). In particular, recent work has shown that the hippocampus can suppress noise in our everyday environment to focus on bottlenecks or sub-goals during multi-step planning (Botvinick & Weinstein, 2014; Stachenfeld et al., 2017). Furthermore, biophysical models predict that the hippocampal theta rhythm can underlie this type of 'sub-goaling' within deep or sequential planning by updating our location from initial starting points to subsequent sub-goals (Kaplan & Friston, 2018), or vice versa (Penny et al., 2013; Kurth-Nelson et al., 2016). Taking this work into account, our data further implicate the hippocampus, and associated theta rhythm, in the restriction of a search space–to focus on bottlenecks during planning (Botvinick and Weinstein 2014, Kaplan et al., 2017b).

Still, several aspects of our results remain unclear. For instance, an alternative explanation for our hippocampal theta power effects could be that there are multiple theta sources (e.g., separate anterior and posterior hippocampal theta rhythms related to accuracy and evaluating demanding upcoming choices) corresponding to the RT and path length effects (Miller et al., 2018), which MEG does not have adequate spatial resolution to resolve. Work comparing potential hemispheric or anterior/posterior differences in the hippocampal theta rhythm may help address this question (Miller et al., 2018). Furthermore, the direct relationship between behaviorally relevant hippocampal theta power changes and the reactivation of place cell sequences is not well characterized, since we are not measuring single-neuron activity. However, Watrous and colleagues (2018) recently observed that human hippocampal single units exhibit phase-locking to the theta rhythm and that this phase-locking encoded information about goal locations during virtual navigation. Work building on this line of research –using hippocampal iEEG recordings to inform whole-brain non-invasive MEG analyses – could provide a novel way to potentially answer questions about the role of the hippocampal theta rhythm in spatial decision-making.

A drawback of our experimental design is that we investigate deep planning in terms of a simple two-level tree search. Because we have a short sequence of choices, we are unable to test whether the hippocampal theta power increases – and behavioural effects related to evaluating subsequent choices – increase with choice sequence length, or only reflect evaluation of the next upcoming choice in a sequence (i.e., next step 'look ahead' behavior). Consequently, investigating the effect of choice sequence length and pruning during planning could help further characterize the underlying computations related to the hippocampal theta changes and behavioral performance observed here (Kaplan et al., 2017a; Keramati et al., 2016; Lee and Keramati 2017).

Notably, we observed human hippocampal theta oscillations partially below the canonical 4-8 Hz theta frequency band, at 3-6 Hz, which is in line with typical observations from direct electrophysiological recordings of the human hippocampus (Jacobs et al., 2014). It is also important to note that we focus on the hippocampal theta rhythm in this study, but

there is a growing literature looking at hippocampal oscillatory coupling with other frequencies (Watrous & Ekstrom, 2014; Lisman & Jensen, 2015; Heusser et al., 2016). Future work could examine how frequency cross-frequency coupling (Lisman et al., 2009) and multiplexing (Akam & Kullman, 2014; Watrous et al., 2013, 2014) maps to different aspects of the planning process.

Our task is reminiscent of perceptual decision-making paradigms and there is an emerging link between saccadic searches and the hippocampus. However, it should be noted that we only measured EOG signals during this task, not saccadic behavior. Future work can build on the growing literature linking visual exploration to movement-initiated hippocampal activity. Of particular interest, Wang and colleagues (2018) found that the firing of single neurons in the human MTL related to successful visual searches for a target item embedded within an image. Moreover, recent studies of the hippocampal formation in humans and non-human primates have related saccadic exploration of visual space to spatial exploration of the physical world (Killian et al., 2012; Jutras et al., 2013; Nau et al., 2018; Julian et al., 2018). Yet, how these findings relate to sequential decision-making/planning remains unclear.

We studied multi-step planning in an explicitly spatial domain, but it is unclear whether updating our 'location' to bottlenecks within a multi-step decision relates more to the overhead visual searches of the maze or a more abstract decision space (Schiller et al., 2015; Kaplan et al., 2017b). On one hand, there is mounting evidence of the type I movement-related rodent hippocampal theta rhythm extending to virtual (Ekstrom et al., 2003, 2005; Watrous et al., 2011; Kaplan et al., 2012; Bush et al, 2017; Watrous et al., 2018) and real-life navigation in humans (Aghajan et al., 2017; Bohbot et al., 2017). However, evidence from other non-spatial domains is lacking. Potential clues may come from the investigation of the role of the hippocampal formation in imagined exploration of spatial environments (Byrne et al., 2007; Bellmund et al., 2016; Horner et al., 2016). Indeed, the hippocampal theta rhythm has been observed during teleportation from one location to another (Vass et al., 2016)– providing further support for a role of the hippocampal theta rhythm in navigating more abstract spaces. Future work exploring the role of the hippocampal theta rhythm in both

perceptual exploration (Jutras et al., 2013; Aronov et al., 2017) and prospective evaluation during abstract sequential decisions (Kaplan et al., 2017b), can determine how generalizable spatial navigation-related hippocampal theta effects are to other abstract spaces (Lisman & Redish, 2009).

In summary, our findings suggest that the human hippocampal theta rhythm plays an important role during spatial decision-making in novel environments. Namely, our data relate hippocampal theta power changes to sequential dependencies during spatial planning. Moreover, we present findings from a spatial decision-making task that more closely resembles perceptual decision-making than virtual navigation paradigms. This therefore leaves open the possibility that the human hippocampal theta rhythm also relates to prospective evaluation during multi-step decisions in non-spatial domains.

References

Aghajan Z, Schuette P, Fields TA, Tran ME, Siddiqui SM, Hasulak NR, Tcheng TK, Eliashiv D, Mankin EA, Stern J, Fried I, Suthana N (2017) Theta Oscillations in the Human Medial Temporal Lobe during Real-World Ambulatory Movement. Curr Biol, 27:3743-51.

Akam T, Kullmann DM (2014) Oscillatory multiplexing of population codes for selective communication in the mammalian brain. Nat Rev Neurosci, 15:111-22.

Aronov, D., Nevers, R., and Tank, D.W. (2017). Mapping of a non-spatial dimension by the hippocampal-entorhinal circuit. Nature *543*, 719-22.

Backus AR, Schoffelen JM, Szebényi S, Hanslmayr S, Doeller CF (2016) Hippocampal-Prefrontal Theta Oscillations Support Memory Integration. Curr Biol, 26:450–7.

Barnes GR, Hillebrand A. Statistical flattening of MEG beamformer images. Hum Brain Mapp. 2003;18:1–12.

Belchior H, Lopes-Dos-Santos V, Tort AB, Ribeiro S (2014) Increase in hippocampal theta oscillations during spatial decision making. Hippocampus, 24:693-702.

Bellmund JL, Deuker L, Navarro Schröder, Doeller CF (2016) Grid-cell representations in mental simulation. Elife, 5:e17089.

Bohbot VD, Copara MS, Gotman J, Ekstrom AD (2017) Low-frequency theta oscillations in the human hippocampus during real-world and virtual navigation. Nat Commun, 8:14415.

Botvinick M, Weinstein A (2014) Model-based hierarchical reinforcement learning and human action control. Philos Trans R Soc Lond B Biol Sci, 369

Bush D, Bisby JA, Bird CM, Gollwitzer S, Rodionov R, Diehl B, McEvoy AW, Walker MC, Burgess N (2017) Human hippocampal theta power indicates movement onset and distance travelled. Proc Natl Acad Sci USA, 114:12297-12302

Buzsáki G & Moser E (2013) Memory, navigation and theta rhythm in the hippocampal-entorhinal system. Nat Neurosci, 16:130-8.

Byrne P, Becker S, Burgess N (2007) Remembering the past and imagining the future: a neural model of spatial memory and imagery. Psychol Rev, 114:340-75.

Cornwell BR, Johnson LL, Holroyd T, Carver FW, Grillon C (2008) Human hippocampal and parahippocampal theta during goal-directed spatial navigation predicts performance on a virtual Morris water maze. J Neurosci, 28:5983-90.

Ekstrom AD, Kahana MJ, Caplan JB, Fields TA, Isham EA, Newman EL, Fried I (2003) Cellular networks underlying human spatial navigation. Nature 425:184-8

Ekstrom AD, Caplan JB, Ho E, Shattuck K, Fried I, Kahana MJ (2005) Human hippocampal theta activity during virtual navigation. Hippocampus **15**:881-9

Fedorov A, Beichel R, Kalpathy-Cramer J, Finet J, Fillon-Robin J-C, Pujol S, Bauer C, Jennings D, Fennessy FM, Sonka M, Buatti J, Aylward SR, Miller JV, Pieper S, Kikinis R (2012) 3D Slicer as an Image Computing Platform for the Quantitative Imaging Network. Magn Reson Imaging 30:1323-41.

Friston K, Buzsaki G (2016) The Functional Anatomy of Time: What and When in the Brain. Trends Cogn Sci, 20:500-11.

Guderian S, Schott BH, Richardson-Klavehn A, Düzel E (2009) Medial temporal theta state before an event predicts episodic encoding success in humans. Proc Natl Acad Sci USA, **106**:5365-70.

Guitart-Masip M, Barnes GR, Horner A, Bauer M, Dolan RJ, Duzel E (2013) Synchronization of medial temporal lobe and prefrontal rhythms in human decision making. J Neurosci **33**:442-51.

Heusser AC, Poeppel D, Ezzyat Y, Davachi L (2016) Episodic sequence memory is supported by a theta-gamma phase code. Nat Neurosci **19**:1374-80

Horner AJ, Bisby JA, Zotow E, Bush D, Burgess N (2016) Grid-like Processing of Imagined Navigation. Curr Biol, 26:842-7.

Jacobs J (2013) Hippocampal theta oscillations are slower in humans than in rodents: implications for models of spatial navigation and memory. Philos Trans R Soc Lond B Biol Sci 369:20130304

Johnson A, Redish AD (2007) Neural ensembles in CA3 transiently encode paths forward of the animal at a decision point. J Neurosci, 27:12176-89.

Jutras MJ, Fries P, Buffalo EA (2013) Oscillatory activity in the monkey hippocampus during visual exploration and memory formation. Proc Natl Acad Sci U.S.A. 110:13144-9.

Kaplan R, Doeller CF, Barnes GR, Litvak V, Düzel E, Bandettini PA, Burgess N (2012) Movement-related theta rhythm in humans: coordinating self-directed hippocampal learning. PLoS Biol, 10:e1001267.

Kaplan R, Bush D, Bonnefond M, Bandettini PA, Barnes GR, Doeller CF, Burgess N (2014) Medial prefrontal theta phase coupling during spatial memory retrieval. Hippocampus, 24:656-65.

Kaplan R, King J, Koster R, Penny WD, Burgess N, Friston KJ (2017a) The Neural Representation of Prospective Choice during Spatial Planning and Decisions. PLoS Biol, 15:e1002588.

Kaplan R, Schuck NW, Doeller CF (2017b) The Role of Mental Maps in Decision-Making. Trends Neurosci, 40:256-59.

Kaplan R, Bush D, Bisby JA, Horner AJ, Meyer SS, Burgess N (2017c) Medial Prefrontal-Medial Temporal Theta Phase Coupling in Dynamic Spatial Imagery. J Cogn Neurosci, 29:507-19.

Kaplan R, Friston KJ (2018) Planning and navigation as active inference. Biol Cybern, Epub Online

Keramati, M., P. Smittenaar, R. J. Dolan and P. Dayan (2016). "Adaptive integration of habits into depth-limited planning defines a habitual-goal-directed spectrum." Proc Natl Acad Sci U S A.

Khemka S, Barnes G, Dolan RJ, Bach DR (2017) Dissecting the Function of Hippocampal Oscillations in a Human Anxiety Model. J Neurosci, 37:6869-76.

Killian NJ, Jutras MJ, Buffalo EA (2012) A map of visual space in the primate entorhinal cortex. Nature, 491:761-4.

Kurth-Nelson Z, Economidies M, Dolan RJ, Dayan P (2016) Fast Sequences of Non-spatial State Representations in Humans. Neuron, 91:194-204.

Lee, J. J. and M. Keramati (2017). "Flexibility to contingency changes distinguishes habitual and goal-directed strategies in humans." PLoS Comput Biol **13**(9): e1005753.

Lega BC, Jacobs J, Kahana MJ (2012) Human hippocampal theta oscillations and the formation of episodic memories. Hippocampus, **22**:748-61.

Lisman J, Redish AD (2009) Prediction, sequences and the hippocampus. Philos Trans R Soc Lond B Biol Sci, 364:1193-201.

Lisman JE, Jensen O (2013) The θ-γ neural code. Neuron, 77:1002-16.

Litvak V, Mattout J, Kiebel S, Phillips C, Henson R, Kilner J, Barnes G, Oostenveld R, Daunizeau J, Flandin G, Penny W, Friston K (2011) EEG and MEG data analysis in SPM8. Comput Intell Neurosci., 2011:852961.

Miller J, Watrous AJ, Tsitsiklis M, Lee SA, Sheth SA, Schevon CA, Smith EH, Sperling MR, Sharan A, Asadi-Pooya AA, Worrell GA, Meisenhelter S, Inman CS, Davis KA, Lega B, Wanda PA, Das SR, Stein JM, Gorniak R, Jacobs J (2018) Lateralized hippocampal oscillations underlie distinct aspects of human spatial memory and navigation. Nat Commun, 9:2423.

Miller KJ, Botvinick MM, Brody CD (2017) Dorsal hippocampus contributes to model-planning. Nat Neurosci, 20:1269-76.

Nolte G (2003) The magnetic lead field theorem in the quasi-static approximation and its use for magnetoencephalography forward calculation in realistic volume conductor. *Phys Med Biol* **48**:3637–3652.

Oehrn C, Baumann C, Fell J, Lee H, Kessler H, Habel U, Hanslmayr S, Axmacher N (2015) Human Hippocampal Dynamics during Response Conflict. Curr Biol, 25:2307-13.

O'Keefe J, Recce ML (1993) Phase relationship between hippocampal place units and the EEG theta rhythm. Hippocampus, 3:317-30.

Olsen RK, Rondina Ii R., Riggs L, Meltzer JA, Ryan JD (2013) Hippocampal and neocortical oscillatory contributions to visuospatial binding and comparison. Journal of Experimental Psychology: General **142**:1335-45.

Oostenveld R, Fries P, Maris E, Schoffelen JM (2011) FieldTrip: Open source software for advanced analysis of MEG, EEG, and invasive electrophysiology data. Comput Intell Neurosci, 2011:156869.

Penny WD, Zeidman P, Burgess N (2013) Forward and backward inference in spatial cognition. PLoS Comput Biol **9**:e1003383.

Pezzulo G, Kemere C, van der Meer MAA (2017) Internally generated hippocampal sequences as a vantage point to probe future-oriented cognition. Ann NY Acad Sci, 1396:144-65.

Poch C, Fuentemilla L, Barnes GR, Düzel E (2011) Hippocampal theta-phase modulation of replay correlates with configural-relational short-term memory performance. J Neurosci **31**:7038-42.

Sarel A, Finkelstein A, Las L, Ulanovsky N (2017) Vectorial representation of spatial goals in the hippocampus of bats. Science 355:176-80

Schiller, D., Eichenbaum, H., Buffalo, E.A., Davachi, L., Foster, D.J., Leutgeb, S., and Ranganath, C. (2015). Memory and Space: Towards an Understanding of the Cognitive Map. J Neurosci. *35*, 13904-11.

Schmidt B, Hinman JR, Jacobson TK, Szkudlarek E, Argraves M, Escabi MA, Markus EJ (2013) Dissociation between dorsal and ventral hippocampal theta oscillations during decision-making. J Neurosci **33**:6212-24.

Stachenfeld KL, Botvinick MM, Gershman SJ (2017) The hippocampus as a predictive map. Nat Neurosci, 20:1643-53.

Staudigl T, Hanslmayr S (2013) Theta oscillations at encoding mediate the context-dependent nature of human episodic memory. Curr Biol, 23:1101-6.

Tauste Campo A, Principe A, Ley M, Rocamora R, Deco G (2018) Degenerate time-dependent network dynamics anticipate seizures in human epileptic brain. PLoS Biol, 16:e20002580.

Vanderwolf CH (1969) Hippocampal electrical activity and voluntary movement in the rat. *Electroencephalogr Clin Neurophysiol*. **26**:407-18.

Vass LK, Copara MS, Seyal M, Shalaie K, Farias ST, Shen PY, Ekstrom AD (2016) Oscillations Go the Distance: Low-Frequency Human Hippocampal Oscillations Code Spatial Distance in the Absence of Sensory Cues during Teleportation. Neuron, 89:1180-86

Villette V, Malvache A, Tressard T, Dupuy N, Cossart R (2015) Internally Recurring Hippocampal Sequences as a Population Template of Spatiotemporal Information. Neuron, 88:357-66.

Wang S, Mamelak AN, Adolphs R, Rutishauser U (2018) Encoding of Target Detection during Visual Search by Single Neurons in the Human Brain. Curr Biol.

Watrous AJ, Fried I, Ekstrom AD (2011) Behavioral correlates of human hippocampal delta and theta oscillations during navigation. J Neurophysiol, 105:1747-55.

Watrous AJ, Tandon N, Conner CR, Pieters T, Ekstrom AD (2013) Frequency-specific network connectivity increases underlie accurate spatiotemporal memory retrieval. Nat Neurosci, 16:349-58.

Watrous AJ, Ekstrom AD (2014) The spectro-contextual encoding and retrieval theory of episodic memory. Front Huma Neurosci, 8:75

Watrous AJ, Miller J, Qasim SE, Fried I, Jacobs J (2018) Phase-tuned neuronal firing encodes human contextual representations for navigational goals. Elife, 7

Wikenheiser AM, Redish AD (2015) Hippocampal theta sequences reflects current goals. Nat Neurosci, 18:289-94.